**Title**
The Effects of a Myocardial Hydrogel on Duchenne Muscular Dystrophy-Associated Cardiomyopathy



**Author**
Fachin, Jade Michelle

**Publication Date**
2022

Peer reviewed|Thesis/dissertation

UNIVERSITY OF CALIFORNIA

Los Angeles

# The Effects of a Myocardial Hydrogel on Duchenne Muscular Dystrophy-Associated Cardiomyopathy

A thesis submitted in partial satisfaction of the

requirements for the degree Master of Science

in Physiological Science

by

Jade Michelle Fachin

2022

ABSTRACT OF THE THESIS

The Effects of a Myocardial Matrix Hydrogel on Duchenne Muscular Dystrophy-Associated Cardiomyopathy

By

Jade Michelle Fachin

Master of Science in Physiological Science

University of California, Los Angeles, 2022

Professor Rachelle Hope Crosbie, Chair

Duchenne muscular dystrophy (DMD) is a progressive, muscle-wasting disease where cell membrane instability continually damages muscle fibers due to an absence of the protein dystrophin. DMD-associated cardiomyopathy is the leading cause of death in patients with DMD and has limited treatment options. Cardiomyocyte death in the heart leads to increased fibrosis, dilation of the cardiac cavities, and decreased contractile function. I am examining the use of a porcine-derived myocardial matrix hydrogel in *mdx* mice, a murine model for DMD, in order to promote extracellular matrix (ECM) remodeling and improve cardiac function. This hydrogel has shown anti-fibrotic effects in the heart post myocardial infarction (MI) in pre-clinical models and a phase I clinical trial. To assess the effects of the matrix hydrogel, I measured the abundance of ECM proteins, quantified macrophage populations and optimized a surgical procedure for echocardiography-guided direct cardiac injection of the matrix hydrogel. We optimized a less invasive protocol for injections and observed a change in the endogenous ECM's architecture.

The thesis of Jade Michelle Fachin is approved:

Amy Catherine Rowat

Melissa J. Spencer

Rachelle Hope Crosbie, Committee Chair

University of California, Los Angeles

2022

DEDICATION

I would first like to dedicate this thesis to my spectacular parents, Arcelia Fachin and Mark Fachin. Your continued support, guidance, and sacrifices are a significant reason why I am able to pursue my dreams. I also dedicate this thesis to my siblings, Adrian Fachin and Xitlalli Bobadilla. You both constantly encourage me to reach new heights. My family continues to be an inspiration and I dedicate this to them.

TABLE OF CONTENTS

LIST OF TABLES AND FIGURES

ACKNOWLEDGEMENTS

I would like to thank Dr. Rachelle Crosbie for her constant guidance and support over two years. Her structured feedback, creative ideas, encouragement, and teaching philosophies have inspired me to improve as a scientist and teacher. Her thoroughness and enthusiasm were key motivators and inspiration to continue my education. I would also like to thank my committee members Dr. Amy Rowat and Dr. Melissa Spencer for their important contributions to my project. Thank you, Dr. Rowat, for your kind wisdom and helpful advice regarding graduate school. Thank you, Dr. Spencer, for providing your expertise and thought-provoking questions which have led me to think critically about my project. Thank you all for being excellent mentors and trustworthy academic sponsors.

I would also like to thank Dr. Jackie McCourt who has shown incredible patience, knowledge, and guidance for over two years. Thank you for your continued wisdom, tenacity, and providing me opportunities to grow as a scientist. This thesis was highly collaborative, and your major contributions helped me navigate this project accordingly. I hope to be as pivotal of a mentor to an emerging scientist as you were to me.

Thank you to all the members of the Crosbie laboratory. Your continued kindness and thoughtful questions have shaped this to be the most challenging yet rewarding experiences. Every member has contributed greatly to my journey, and I am grateful to contribute among a group of intelligent individuals. I also want to thank Dr. Karen Christman and her laboratory for creating and providing the hydrogel used in this study.

This study was made possible by the following grants: NIH NIAMS R01 #AR048179 and NIH NHLBI R01 #HL126204

## BACKGROUND

Duchenne muscular dystrophy (DMD) is an X-linked disease that is diagnosed by the absence of the dystrophin protein. The dystrophin protein is an integral structural link to intercellular actin, transmembrane proteins, and the extracellular matrix (ECM). The DMD gene that encodes dystrophin contains 79 exons and is the largest gene in a human[1]. A premature stop codon in this gene leads to DMD. However, other mutations, such as single nucleotide polymorphisms, can lead to milder diseases like Becker's muscular dystrophy[1]–[3]. Dystrophin is a component to the Dystrophin-Glycoprotein Complex (DGC). The DGC has intracellular, transmembrane, and extracellular components. Some intracellular components include actin and dystrophin. There are transmembrane proteins such as sarcospan, sarcoglycans and alpha dystroglycan. Extracellularly there is beta dystroglycan which attaches to laminin. This attachment to laminin is the DGC's link to the ECM whereas dystrophin binding to actin filaments serves as an intracellular link[4].

Without dystrophin, the muscular sarcolemma is more susceptible to contraction-induced injuries. An accumulation of these injuries results in muscle cell death, rendering them weaker with each injury[5]. This leads to systemic muscular weakness and eventual fatality from respiratory or cardiac failure. DMD is a chronic, progressive muscle wasting disease that affects every muscle in the body. Muscular weakness can be seen clinically at a few years old[6]. There is a major importance in an early diagnosis. Equally important is implementing the necessary precautions and medicines tailored for each patient. Skeletal and cardiac muscle in a DMD context have been researched intensively, however, this thesis will be in the context of cardiac muscle. Cardiac fibrosis typically precedes cardiomyopathy. Fibrosis is a common pathology for many cardiomyopathies[5]. The left ventricle will receive multiple tears along the cardiomyocyte

sarcolemma. Continued tears lead to an accumulation of scar tissue along the ventricular walls. As the disease progresses, cardiomyocytes are unable to regenerate as efficiently. The ventricular walls inevitably become stricken with scar tissue. Although the ventricle becomes increasingly more dilated, the muscles are weaker and there is less pressure to push the blood throughout the body. Due to continued scientific advancements in respiratory treatments (i.e., ventilators), patients are living longer. However, DMD pathology includes a chronic development of cardiomyopathy thus there is an overwhelming need to mitigate DMD-associated cardiomyopathy. By optimizing a cardiac treatment in the context of DMD, similar cardiomyopathies can also benefit from a potential anti-fibrotic change in the endogenous matrix post injection.

A current typical gold standard of treatment for DMD-associated cardiomyopathy includes steroids (typically Prednisone or Deflazacort) starting from an early age, Angiotensin Converting Enzyme Inhibitors (ACE-Is), and diuretics[6], [7]. These medications aim to mitigate the sympathetic nervous response and overworking of the heart. As the disease progresses, the heart chambers gradually dilate, leading to an increased volume. However, the muscles waste and are replaced by scar tissue, which are not as effective at pumping blood systemically. The heart becomes weaker which leads to lower blood pressure. This decrease in blood pressure causes a homeostatic response to raise blood pressure by making the heart pump faster. This can be incredibly damaging for individuals with DMD since overworking cardiomyocytes leads to contraction-induced tearing and a weaker heart.

There have been many bioengineering innovations regarding building scaffolds of matrix treatments. Some injectable matrices have been chemically and organically made[8], [9]. Karen Christman’s lab at University of California, San Diego developed a novel matrix hydrogel from

decellularized healthy porcine myocardium. To generate the matrix hydrogel, they harvested the left ventricles of healthy pig hearts, cut them into small pieces, decellularized the tissue, lyophilized then milled the tissue, then resolubilized the milled powder into a viscous gel by enzymatic reactions[10]. The hydrogel was optimized for optimal delivery via catheter or syringes[11], [12]. To test their hydrogel, they performed surgeries on rat and pig models of myocardial infarction. In these models, the myocardial matrix hydrogel has shown to promote a remodeling environment in the heart post myocardial infarction. Some of their findings included lower interstitial fibrosis, increased blood vessel formation, a change in the immune response, and decreased apoptosis[13]. Given the success of the Christman lab's experiments, we sought to determine whether the hydrogel alters the endogenous ECM environment of DMD-associated cardiomyopathy. Investigating the effects of the myocardial matrix hydrogel in a dystrophic heart can elucidate the translational potential of the hydrogel and provide a new therapeutic approach in the treatment of DMD-associated cardiomyopathy.

# CHAPTER 1: TO TEST THE PHYSIOLOGICAL AND CLINICAL APPLICATIONS OF A MYOCARDIAL MATRIX HYDROGEL IN A MOUSE MODEL OF DMD

## Introduction

The hydrogel has shown success in improving the endogenous extracellular matrix environment post-myocardial infarction (MI) in rats, pigs, and human hearts[11], [14], [15]. Although MI is an acute injury to the heart and dilated cardiomyopathy in muscular dystrophy is a chronic, progressive degeneration, the hydrogel could exhibit a similar benefit in a more progressive cardiac injury context. The hydrogel injection surgical procedure has been optimized in rats, pigs, and humans by the Christman lab. However, a murine model of DMD, the *mdx* mouse, has not yet been used for hydrogel delivery and analysis. Given the size difference between rats and mice and the sensitivity of the *mdx* mouse to stress, we sought to optimize a surgical procedure for direct cardiac injection of a hydrogel in *mdx* mice. In order to test the clinical potential of the hydrogel, there is a necessity for a protocol that optimizes survival of the animal and allows for precise injection of the hydrogel into the myocardium where fibrosis is evident.

Delivering the hydrogel directly into the left ventricle requires precision and accuracy. Our first approach to hydrogel delivery utilized a mouse thoracotomy procedure. This surgery requires intubation of the mouse, opening the chest cavity, and exposing the entire heart. Once the heart was exposed, we were able to directly inject 5-10 µl of hydrogel into the left ventricular wall. This procedure yielded a 50% survival rate as seen in Table 1.1 and Table 1.2, mostly due to surgical or direct cardiac injection complications. To improve survivability, we turned to an echo-guided procedure that uses ultrasound imaging to guide the needle directly to the left ventricular wall without having to open the thoracic cavity. With an increased survivability,

physiological data (i.e., Echocardiographs) can be measured pre-, peri- and post- procedure. This aim compared data between the mouse thoracotomy and the echo-guided injection surgeries to optimize delivery of the hydrogel.

The mouse used in this study, the *mdx* mouse, typically shows a dilated cardiomyopathy phenotype by 12 months but shows prominent fibrosis by 5 months of age. Due to time limitations, it was not feasible to use mice at 12 months. Instead of aging the mice to 12 months, we can stress the mouse heart at 5 months using an isoproterenol challenge in order to reveal an earlier physiological phenotype[16]. Previous studies on *mdx* mice show a clear physiological stress on the heart post isoproterenol challenge compared to wild-type mice[16]. This stress was seen by increased heart rate, increased left ventricular fractional shortening, and increased left ventricular ejection fraction. In future studies, using echocardiographs pre- and post-challenge, after optimization of the hydrogel injection procedure will aid in examining whether the hydrogel protects the heart from an isoproterenol challenge. Protection will be measured and analyzed through changes in physiological parameters obtained by echocardiographs in order to demonstrate the hydrogel's clinical potential.

## Materials and Methods

### Animals

In the study, *mdx* mice were obtained from Jackson Laboratories and maintained by *mdx* x *mdx* crosses. Mice were aged to 5 months for the hydrogel procedures. Mice were maintained in the Terasaki Life Sciences Vivarium, and all procedures were carried out in accordance with the Institutional Animal Care and Use Committee (IACUC) at the University of California, Los

Angeles guidelines. Open thoracotomy surgical procedures and echocardiographs were carried out in the Physiology Core at UCLA.

Hydrogel

The hydrogel was made by Dr. Karen Christman's lab at University of California, San Diego[16]. The Christman Lab engineered a matrix hydrogel from decellularized healthy porcine hearts. The ventricular ECM was lyophilized, milled to a powder, and enzymatically digested to become a liquidized gelation[11]. The solubilized hydrogel could be kept on ice or in a freezer, ready to use. Hydrogel was kept frozen in-house at -80°C with a shelf life of six months. For hydrogel injections, the lyophilized powder was reconstituted in water and serially pipetted through needles of increasing gauges (27G, 29G, 31G). Direct cardiac injection of the hydrogel was done using a 31G needle with ¼ inch (open thoracotomy) or 1 inch length (echo-guided).

Mouse thoracotomy

Mice were anesthetized in an induction chamber with 2% isoflurane mixed with 0.5-1.0 L/min 100% $O_2$ and during the surgical procedure was maintained at 1.5-2.0 L/min 100% $O_2$. Mice were intubated, ventilated and normal body temperature was maintained via a circulating water pad. Partial thoracotomy to the fifth rib was performed to expose the ventricular wall for direct cardiac injection. The rib cage was closed with 6.0 prolene suture using an interrupted suture pattern flowed by suture of the overlying skin. Post-operative analgesia Buprenorphine (0.1 mg/kg) was interperitoneally administered. Mice were monitored for signs of dehydration and distress.

Echo-guided surgeries

Echocardiograms for the echo-guided injections were done using a Vevo 3100 Visual Sonic imaging system with a MC2505 probe, courtesy of Dr. Pearl Quijada's lab at UCLA. Mice were anesthetized with 2% isoflurane mixed with 0.5-1.0 L/min 100% $O_2$ and during the surgical procedure was maintained at 1.5-2.0 L/min 100% $O_2$ through a nose cone. Mice were kept warm on the imaging table at 37°C. Hair was removed on the chest using hair removal cream and ultrasound gel was applied to the chest area. Both long and short axis views were obtained with the long axis view being the best view for cardiac injections into the cardiac wall. Once a clear long axis view was obtained, the needle was aligned with the probe and viewed by the ultrasound using a needle guide feature in the Vevo 3100 software (Figure 1.1A-B). Saline, hydrogel, and Evan's blue dye were used in our practice injections. The volumes for saline and Evan's blue dye were 50-70 uL in order to visualize the injection and identify the site of injection post-mortem. The volume of hydrogel used was 10 uL for practice injections.

Echocardiogram measurements

Echocardiograms for the echo-guided injections were done using a Vevo 3100 Visual Sonic imaging system with a MC2505 probe. Images of the long-axis view and short axis view in doppler and B-mode were taken in order to get measurements of wall thickness, left ventricular ejection fraction and fractional shortening, and systolic and diastolic diameters. These measurements were taken immediately before and after the injection.

Statistical Analysis and Figures

Figures and statistical tests were done using Graph 8 Prism software. Figures were generated in Microsoft PowerPoint.

## Results

By optimizing a protocol we were able to visualize the injection site to ensure proper delivery to the left ventricular wall and allow for a quick post-recovery in the mice (Figure 1.1A-B). Visualization of the injection was done during the injection using the echo imaging system, but also done post-mortem when harvesting the hearts. We added Evan's blue dye into the saline mix in the syringe for two 9-month-old male *mdx* mice. Hearts were immediately harvested and cryopreserved after the injection. The Evan's blue dye was visualized on unstained serial sections of the heart under bright field microscopy (Figure 1.1C-D).

## Discussion

The initial procedure for delivering the hydrogel was through a mouse thoracotomy. Two sets of male *mdx* cohorts underwent the mouse thoracotomies. There were many difficulties with this invasive procedure and most of the deaths were from surgical complications. Some of these complications included difficulty with intubation, bruising, heart block, and stitching. The list of the 2019 cohort mice can be seen in Table 1.1 and the 2021 cohort is listed in Table 1.2. These tables show which injection (saline or hydrogel) the mice had, how much was injected, whether they survived, and if they died, a cause of death was given.

While developing the protocol, we performed several practice echo-guided surgeries and injections. The main goal of optimizing a protocol was becoming familiar with the equipment, maintaining animal ethical practices, acquiring images and orientations suitable for cardiac wall injection, and improving survival rate for physiological analysis. Using an echocardiography imaging system, we were able to visualize the needle, the left ventricular wall, and injection in real time. The echocardiography imaging system allowed us to project a long axis view of the

left ventricular wall. We attempted to replicate a similar angle of injection and view on the echocardiogram before each injection. Although there were many components and nuances for each mouse, we were able to visualize the injections. We were able to perform multiple saline injections on male and female *mdx* mice at varying ages. The majority of the mice survived and were able to undergo a second injection. We determined that it is necessary to use a new needle after every two injections to maintain a sharper needle point for insertion into the chest cavity. One important point of this injection is to ensure proper delivery into the left ventricular wall. An accidental injection of the hydrogel into the left ventricular cavity could be fatal. The echo machine greatly assisted in showing the depth of the needle prior to injection.

Visualizing and taking measurements of the heart at many angles gave us an idea of what the state of the heart was and if there were any abnormalities. For the injection, the echo probe had to be parallel with the needle tract in order for a clear visualization of the needle. Ensuring the needle was visible as it entered the heart was a key component of this aim. There were some difficulties if there was an unknown obstruction near the heart that prevented clear imaging prior to injection. If there was not a clear view of the heart and needle, we did not inject into that mouse.

Evan's blue dye was utilized as a means of further visualization of the site of injection post-mortem. A secondary reason for using Evan's blue dye is that it could be a useful tool in future experiments to determine the extent of membrane damage to the cardiomyocytes since the dye is membrane impenetrable except when the membrane is damaged. Since membrane damage is a profound component in DMD, it was an appropriate dye for visualization during the echo and after sacrificing the mouse. Future directions could investigate the use of India ink as another means of visualizing the site of injection.

# CHAPTER 2: EFFECTS OF MATRIX HYDROGEL ON ECM REMODELING OF DMD-ASSOCIATED CARDIOMYOPATHY

## Introduction

One of the primary fatalities in DMD is dilated cardiomyopathy (DCM). DCM pathogenesis stems from the left ventricle, the chamber which sends blood systemically after contraction. Unlike skeletal muscle, the heart's regenerative capacity greatly diminishes after the fetal stage of mouse development and an injury will result in the generation of a fibrotic scar or lesion[17]. The dystrophic heart will develop sarcolemma damage and cardiomyocyte death over time that is replaced by deposition of ECM. Although fibrosis is a physiological response necessary to maintain contractile function of the heart, accumulated scar tissue can be pathological overtime and can contribute to inefficient cardiac function. The heart's overall health declines and is reflected by a larger end diastolic volume and lower ejection fraction. The left ventricle will dilate, cardiomyocytes will not regenerate and the ventricular walls line with fibrotic tissue.

The extracellular matrix (ECM) is a complex scaffold responsible for signaling transduction and structural support for resident cells. A continuously injured heart will accumulate fibrosis thus weakening the heart's overall function. Although the adult mouse heart has limited regenerative capabilities, the myocardial matrix hydrogel has demonstrated improved ECM remodeling at the site of MI injury. Aim 2 of my thesis focused on investigating whether the hydrogel can also promote remodeling of the matrix by measuring changes in fibrotic protein markers and collagen degradation. The two main ECM proteins investigated were collagen I and fibronectin. Fibronectin is an ECM glycoprotein component found in the basement membrane that binds to integrins and laminin. Fibronectin has a role in communication between cells,

prevents myoblast differentiation, and is mainly secreted by fibroblasts. Fibronectin and collagen I have been found to increase in diseased hearts[18]–[20]. This was rationale to investigate these extracellular components for this project. By evaluating various components of the ECM and cellular responses, we can evaluate the remodeling capabilities of the hydrogel on *mdx* mouse hearts.

## Materials and Methods

### Animals

Six 5-month-old *mdx* mice were used for this set of tissue analysis. 4 of the mice were injected with the matrix hydrogel, and 2 injected with saline. In the study, *mdx* mice were obtained from Jackson Laboratories and maintained by *mdx* x *mdx* crosses. Mice were aged to 5 months for the hydrogel procedures. Mice were maintained in the Terasaki Life Sciences Vivarium, and all procedures were carried out in accordance with the Institutional Animal Care and Use Committee (IACUC) at the University of California, Los Angeles guidelines. Open thoracotomy surgical procedures and echocardiographs were carried out in the Physiology Core at UCLA.

### Hydrogel

The hydrogel was made by Dr. Karen Christman's lab at University of California, San Diego[16]. The Christman Lab engineered a matrix hydrogel from decellularized healthy porcine hearts. The ventricular ECM was lyophilized, milled to a powder, and enzymatically digested to become a liquidized gelation[11]. The solubilized hydrogel could be kept on ice or in a freezer, ready to use. Hydrogel was kept frozen in-house at -80°C with a shelf life of six months.

### Hydrogel Injection

Injected either once or twice in the left ventricle to the *mdx* mice at 4 weeks of age with a 31G, ¼ inch needle, insulin syringe. The singular doses contained 4-5 μL hydrogel or saline. The double doses contained 4-6 μL hydrogel or saline. Singular doses were done in the mid-ventricular region. Double doses were injected at the apex myocardium and mid-ventricle myocardium.

Histology

The cryopreserved hearts were serially sectioned in a Leica cryostat at -23ºC at 10μM thickness, from the base to the apex. Slides were stained with hematoxylin and eosin and Masson trichrome according to the manufacturers protocol. Hematoxylin and eosin stains were done on various slides throughout the heart to identify the approximate location of the hydrogel injection. Once the hydrogel injection site was identified, adjacent tissue slides were chosen for Masson trichrome and subsequent indirect immunofluorescence analysis.

Indirect Immunofluorescence

Antibodies against collagen I (1:250, Cedar Lane # CL50151AP-1) and fibronectin (1:250, Abcam # ab2413) were used for indirect immunofluorescence of ECM proteins. For macrophage stains, CD206 (Biorad # MCA2235) was used to measure M2 levels whereas CD68 (BioRad # MCA1957) was used to measure M1 levels. Collagen hybridizing peptide (CHP) antibodies were used to measure denatured collagen levels (3Helix # FLU300) The tissues were imaged on a Zeiss Axio Imager M2 microscope using Zen blue edition software. ImageJ was used to quantify the images using Corrected Total Fluorescence. The fluorescence was quantified from an entire image mosaic, taken from a sum of individual tiles. The Masson's trichrome stain quantification was done by measuring the amount of blue stain present in the tissues.

Statistical Analysis and Figures

Figures and statistical tests were done using Graph 8 Prism software. Figures were generated in Microsoft PowerPoint.

**Results**

To identify the site of injection in the harvested tissue, we took H&E stains in a series of every 300 μm of tissue. The serial H&E stains aided us in identifying the approximate location of the injection site indicated by area of white and pink staining. Slides around this identified injection site were used for indirect immunofluorescence and other histology. The Masson trichrome stain is nonspecific for collagen and thus indicates areas of increased collagen deposition (Figure 2.1). There were tissue slides taken adjacent to the injection site and two taken non-adjacent to the injection site for each mouse in the first cohort. Quantification of the Masson trichrome indicates an increase in collagen in hydrogel injected hearts at the adjacent site (Figure 2.2).

To assess the amount of matrix deposition and remodeling, we measured collagen I and fibronectin protein levels using indirect immunofluorescence. Collagen I is the most abundant fibrillar protein in the ECM[21]. It is responsible for providing tensile strength for cardiomyocytes. Masson's trichrome is a preliminary stain that is non-specific for collagen fibrils and gives an approximate view of the fibrotic state of the tissue. To gain specificity, collagen I was stained using indirect immunofluorescence (Figure 2.3A-B). Similar to the Masson trichrome stain, we wanted to compare collagen I detection at the injection (adjacent) versus the non-adjacent sites. The non-adjacent sites were taken in equal distance from the adjacent site. One being more toward the base, while the other being more toward the apex of the

mouse heart (Figure 2.4). However, to elucidate further on the state of the collagen I, we utilized a collagen hybridizing peptide (CHP) to see denatured collagen (Figure 2.5). CHP has a strong affinity to bind to denatured collagen[22]. Although fibrosis is a physiological process in the response to cardiac injury, fibrosis can also become pathological. Since there are pathological and physiological fibrotic responses, our goal included utilizing CHP to visualize how collagen was conforming itself. For fibronectin, there seemed to be an increase near the injection site in the hydrogel injected tissues (Figure 2.6). There was a slight increase in fibronectin levels in the hydrogel injected mice compared to the saline injected mice (Figure 2.6C).

Prior studies done at the Christman lab showed a change in the immune response. This was rationale to perform a similar analysis in my project, but with an addition of M2 populations (Figure 2.7).

**Discussion**

There was a trend of extracellular matrix remodeling post-hydrogel injection. A possible reason for this behavior could be due to the heart's response to the traumatic surgery. The cardiac tissues analyzed in this aim were the cardiac tissues that underwent the mouse thoracotomy and harvested 2 weeks post-injection. We chose to initially utilize the mouse thoracotomy protocol along with this harvesting timeline which was similar to a previous hydrogel study on a rat model[23], [24]. The heart has limited healing capacities past the fetal age and the heart may require a longer time to heal post-surgery.

There was an increased fibrotic environment observed in the Masson trichrome (Figure 2.1), collagen I (Figure 2.3) and fibronectin (Figure 2.6) stains along with their quantifications. Along with an increased level of these extracellular proteins, we observed a greater spread of the

data among the hydrogel injected mice. The hydrogel seemed to promote a change in the endogenous ECM architecture measured in this study with an upward trend of the specified proteins. This increased fibrotic environment could be a natural healing response from the invasive mouse thoracotomy surgery. Another reason for this increase, could be that the left ventricle is in the process of rebuilding itself. Since the heart has limited regenerative capacity, the healing process could be delayed, especially in diseased mice. We cannot say whether this is a beneficial or pathological increase in fibrillar proteins until further studies are conducted. Further studies with the less invasive echo-guided injection (discussed in Specific Aim 1) and/or a longer healing time post-surgery may aid in a more definitive conclusion on whether the hydrogel promotes an anti-fibrotic endogenous ECM environment post-injection and overall heart efficacy.

A speculation was raised regarding the increasing matrix proteins after the injection. We are injecting a matrix scaffold derived from a healthy decellularized porcine heart into the left ventricle, so it is logical to conclude there would be a higher amount of the ECM proteins being analyzing. The Christman lab has determined in previous experiments that most of the hydrogel will dissipate within a week[12]. That study also found one rat heart to have slight hydrogel present at 14 days, with complete dissipation of the hydrogel at 28 days. This is an important note to keep in mind for further studies and for extending the harvesting timeline to 4 weeks instead of 2 weeks.

The purpose of this matrix hydrogel is to promote change in the endogenous ECM environment through this injectable scaffold. We wanted to compare collagen levels that were equal but opposite directions from the injection (adjacent) site. We analyzed Masson trichrome and collagen I stain on tissues non-adjacent to the injection site. Analyzing tissues that were

located more toward the base or the apex of the heart allowed us to compare localized (in terms of the hydrogel injection) collagen I levels and non-adjacent areas of the same heart. In the Masson trichrome and the collagen I non-adjacent quantifications, the base non-adjacent sites showed no significance. However, interestingly, both apex non-adjacent sites showed a significant difference between saline and hydrogel injected tissues (Figure 2.2 and Figure 2.4). The apex non-adjacent tissues displayed a higher amount of Masson trichrome and collagen I quantifications. The apex of the heart represents a lower area of the left ventricle than where the injection site was. A reason for these changes in the endogenous ECM proteins could be the hydrogel's scaffold permeated more through the lower area of the heart than the upper half. An increase in the scaffold availability may allow for increased remodeling activity and therefore an increase in fibrillar proteins. Although we are identifying this as a change in the ECM proteins, we are seeing upward trend. However, we cannot definitively conclude this as beneficial or detrimental to heart efficacy at this stage. These findings allow for further questions and considerations to be raised for future studies, including ensuring a consistent angle of injection (which the echo machine has assisted with along with a "Needle Guide" feature). It is important to note a few *mdx* cardiac tissues were excluded from the apex non-adjacent quantification due to blurred images.

Another prominent question asked in this study involves differentiation between intact vs denatured collagen. Especially after observing an increase in fibrillar proteins 2 weeks post-hydrogel injection, one being the collagen I IFA stain (Figure 2.3). To assess further into the state of the collagen, we looked at a collagen hybridizing peptide (CHP) stain (Figure 2.5). The stain will bind to incomplete/denatured collagen fibrils[22]. A higher amount of CHP levels could indicate more denatured collagen. Since this was a new stain in our laboratory, we wanted

to test its efficiency. The two mouse cardiac tissues used were DBA *mdx* and wild-type. Although not quantified, we saw a higher level of CHP stain in the DBA *mdx* tissues (Figure 2.5). This makes sense since the DBA *mdx* model is a more severe form of the *mdx* model. We stained the two models with collagen I as a comparison to see if the stain was detecting the appropriate locations. The CHP stain was able to faintly detect overlapping collagen locations compared to the collagen I stain (Figure 2.5).

It is also important to note that although this hydrogel was derived from a porcine heart, ECM proteins are highly conserved across mammalian species. There has not been a rejection of this hydrogel in rats, pigs, humans from previous studies[10], [12] and now mice.

Future directions will include experiments with a longer time post-injection before harvesting. In this study, we harvested the hearts 2 weeks post-injection utilizing the mouse thoracotomy surgical procedure. Since this method is an invasive, physically traumatic procedure, perhaps the recovery may take a bit longer. If the harvesting happened at 4 weeks instead, maybe the hearts' endogenous extracellular matrix would have more time to remodel, potentially trending toward an anti-fibrotic environment. Extending the recovery time also extends when the mice are sacrificed. In this extended time we can elucidate on the hydrogel's longer-term effects on the heart. With a longer duration post-hydrogel injection, we can take echocardiograms and induce a beta-isoproterenol challenge to gain further physiological data and determine whether the hydrogel provides protection against beta-isoproterenol stress. The isoproterenol challenge has been done in prior studies in *mdx* mice and demonstrated that the *mdx* mice are particularly susceptible to stress on the heart[16]. Our lab had previously tested the isoproterenol challenge on *mdx* mice and found a decrease in heart function after a single trial run. The protocol used in our lab was used in Yue et al's protocol described in their study[16].

The Christman lab saw a change in the inflammatory response of the heart post-MI and hydrogel injection in rats and more specifically an increase in the M1 macrophage population[12], [13], [25]. Although the results they found were not significant, there was still a change in the immune response detected. This was rationale to perform a similar analysis in my project, but with an addition of M2 populations. In our study, there were some preliminary M1 and M2 macrophage phenotype analysis. We observed a larger ratio of M1 phenotype to M2 phenotype (Figure 2.7). Although this was a preliminary assay, we did see an increase in M1 population. We cannot make conclusions at this time and will need to investigate the immunological response to the hydrogel further for complete analysis.

Now that we have optimized a less invasive approach for cardiac injection in mice, this will improve survivability. Improving survivability will allow us to further analyze tissue samples and stains post-injections. With more animals available to study, we will be able to separate the effects of the hydrogel injection from natural variability. Future directions include utilizing the same indirect immunofluorescence assays and histology stains used in this aim but with mice that have undergone echo-guided injections rather than thoracotomies. With an optimized delivery of the hydrogel on a mouse model, this expands the number of animals able to be tested with the hydrogel. The echo-guided injection provides a visual of the heart, ability to collect echocardiograms before, during, and after the procedure. This has had a significant survival rate increase compared to the invasive mouse thoracotomy approach. An accumulation of data that analyzes the different surgical approaches and extended time until heart harvest will provide a more comprehensive understanding of the effects from the hydrogel on the endogenous ECM in *mdx* mice.

Another important question to ask is how the hydrogel acts in a wild-type (WT) mouse. This is a recognized limitation of this project. The control of our experiments in this study was the saline injection, but all injections and analysis were performed on *mdx* mice at similar ages. The *mdx* mouse model is a diseased model with its own pathological timeline. These mice may have difficulty repairing their injuries comparatively to WT mice. Injecting saline or hydrogel on a WT mouse will elucidate further into a baseline ECM response and comparing survivability of the mouse thoracotomy with WT mice.

## CONCLUSION

This study's main goal was to develop a feasible protocol for injecting a porcine-derived hydrogel to *mdx* mice and investigating the effects of the hydrogel on endogenous cardiac ECM. We observed an overall increase in fibrosis related proteins including collagens, collagen I, and fibronectin. These results raise questions on whether the hydrogel affects the heart in the long term and if the hydrogel protects the heart's contractile dysfunction. The hydrogel has shown anti-fibrotic properties in skeletal muscle *mdx* mouse models and other animal models with ameliorating pathological effects post-injury. This study provides a crucial foundation for future research into the hydrogel's clinical potential for DMD-associated cardiomyopathies and similar pathologies.

Future directions to further analyze the potential of the hydrogel in DMD-associated cardiomyopathy should include a utilization of the optimized echo-guided protocol for delivery and determine whether the hydrogel provides any physiological benefit to *mdx* mice. By inducing a less invasive approach when delivering the hydrogel, this prompts further physiological studies (i.e. echocardiograms and isoproterenol challenges) and histological studies of the cardiac tissue. We were able to devise a successful protocol that improved survivability, maintained constant visuals of the heart, and required less analgesics for a quick recovery. Another future direction could be to investigate the hydrogel's physiological effects in response to other stresses such as an exercise regime[26], [27]. This will exacerbate the heart's pathology and more accurately mimic human clinical presentation of DMD-associated cardiomyopathy. A more in-depth analysis into these questions will elucidate further on optimizing the hydrogel's delivery methods and a potential therapeutic approach to cardiomyopathy that stretches beyond DMD.

## TABLES AND FIGURES

| Mouse | Injection | Status |
|---|---|---|
| mdx #1 (2019) | 2 hydrogel inj. (~50ul total); wrong needle | Heart block after 2nd injection |
| mdx #2 (2019) | 2 10ul hydrogel inj. | Heart block after 2nd injection |
| mdx #3 (2019) | 2 4-6ul hydrogel inj. at apex and mid-heart | Survived; sac'd at 2 weeks, heart collected |
| mdx #4 (2019) | 2 4-7ul hydrogel inj. | Bruise developed at site of 1st injection; died during suturing |
| mdx #5 (2019) | Surgery complication | Died during surgery before inj. |
| mdx #6 (2019) | 1 5ul hydrogel inj. | Died after suture; bruised at site |
| mdx #7 (2019) | 2 4-6ul saline inj. | Survived; sac'd at 2 weeks, heart collected |
| mdx #8 (2019) | 1 5ul hydrogel inj. | Survived; sac'd at 2 weeks, heart collected |
| mdx #9 (2019) | 1 5ul hydrogel inj. | Survived; sac'd at 2 weeks, heart collected |
| mdx #10 (2019) | 1 4ul hydrogel inj. | Survived; sac'd at 2 weeks, heart collected |
| mdx #11 (2019) | 1 5ul saline inj. | Survived; sac'd at 2 weeks, heart collected |

**Table 1.1: The 2019 Cohort of 5-Month-Old Male *mdx* Mice.** Rows highlighted in yellow indicate mice injected with the matrix hydrogel. Rows highlighted in green indicate mice that were given a saline injection.

| Mouse | Injection | Status |
|---|---|---|
| mdx #1 (2021) | No injection | Died after intubation prior to injection; heart collected |
| mdx #2 (2021) | No injection | Died before intubation; heart collected (hypertrophy evident) |
| mdx #3 (2021) | Hydrogel injection, 2 4ul injections (first one leaked out) | Survived; collected heart at 2 weeks post -injection |
| mdx #4 (2021) | Hydrogel injection, ~7 ul (some leaked) | Died during suturing, no evident bruising |
| mdx #5 (2021) | Saline injection, ~7ul | Survived; collected heart at 2 weeks post -injection |
| mdx #6 (2021) | Hydrogel injection, ~7ul | Died after injection; heart collected (hypertrophy evident) |
| mdx #7 (2021) | Hydrogel injection, ~7ul | Survived; collected heart at 2 weeks post -injection |
| mdx #8 (2021) | Hydrogel injection, ~7ul | Survived; collected heart at 2 weeks post -injection |
| mdx #9 (2021) | Saline injection, ~7ul | Survived; collected heart at 2 weeks post -injection |
| mdx #10 (2021) | No injection | Tear in trachea, died during intubation |

**Table 1.2: The 2021 Cohort of 5-Month-Old Male *mdx* Mice.** Rows highlighted in yellow indicate hydrogel injected mice, whereas rows highlighted in green indicate saline injected mice.

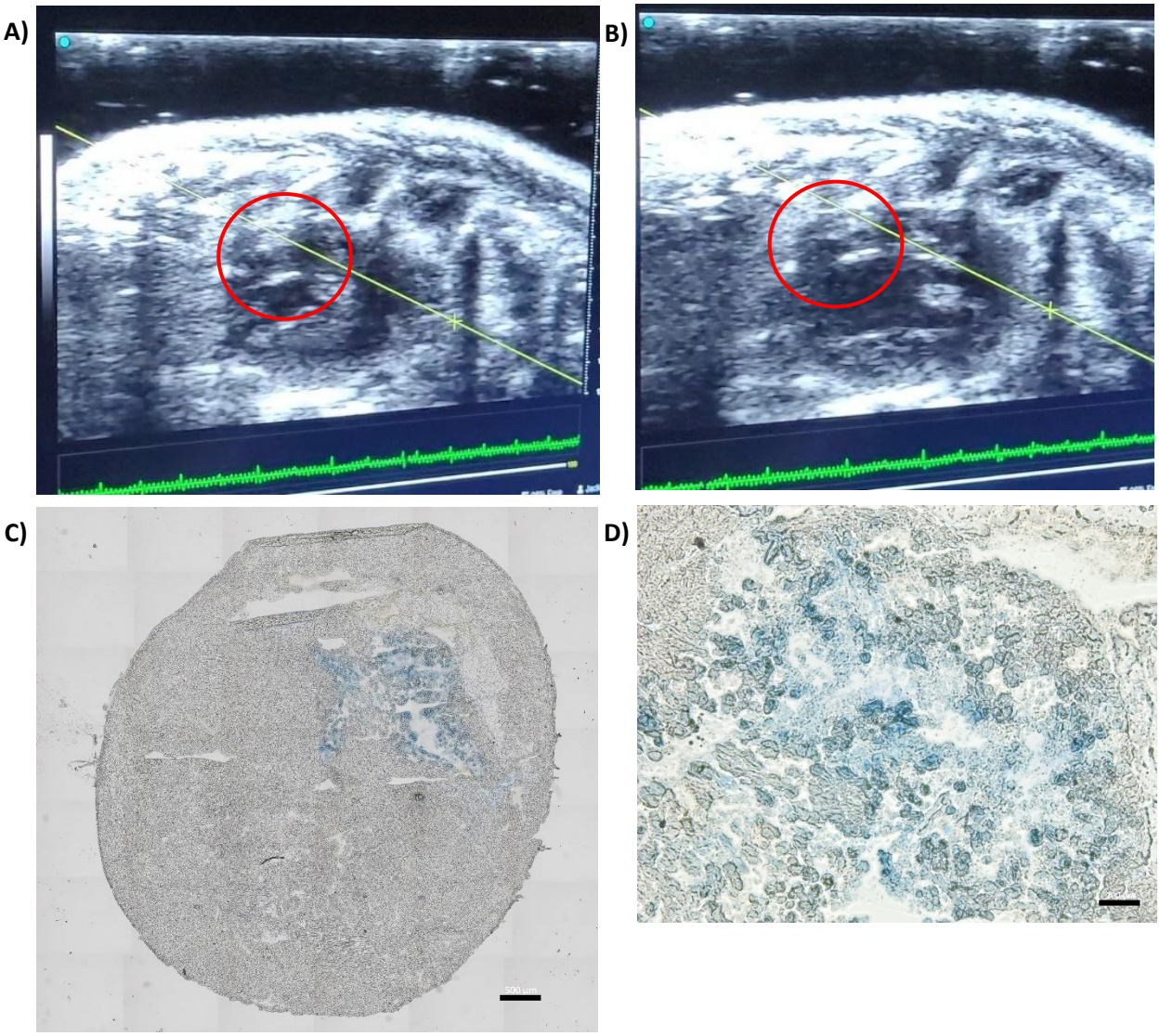


**Figure 1.1: Utilizing Echo-guided Injections for Hydrogel Delivery to Mice Hearts**. **(A)** An echocardiography where the needle can be seen in the left ventricular wall. The red circle shows the needle. The green line is a needle injection guide used for consistent angle of injection. **(B)** An echocardiography from the same heart as (A), but right after the needle was removed from the ventricular wall. **(C)** An unstained cardiac tissue. The blue in the ventricular cavity indicated the Evan's blue dye injected into practice *mdx* hearts. Scale bar at 500um. **(D)** A close-up of (C), highlighting the Evan's blue dye. Scale bar at 100um.

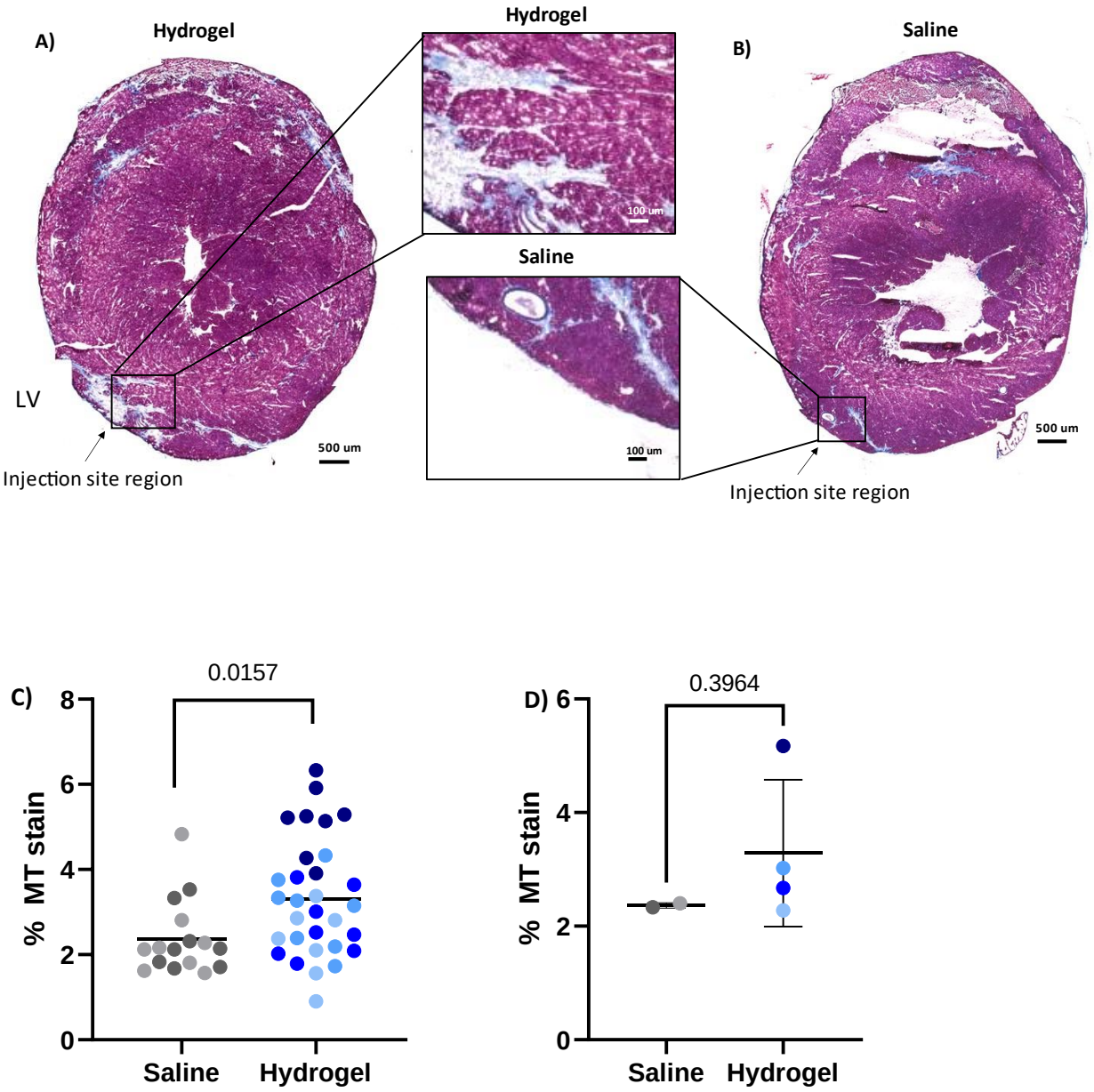


**Figure 2.1: Increased Masson Trichrome Stain in Hydrogel-Injected Tissues. (A)** A mosaic image from the hydrogel injected heart tissue. Zoomed in picture shows a close-up of the approximate injection site region in the left ventricle (LV). **(B)** Mosaic image from the hydrogel injected heart tissue. Zoomed in picture shows a close-up of the approximate injection site region in the left ventricle. **C)** Each quantification from the tissues. Each mouse has 4 quantifications from 4 tissue sections. **D)** Quantification of the average percentage Masson trichrome stain. n = 2 saline injected mice, n = 4 hydrogel injected mice. Unpaired t test statistical analysis was performed.

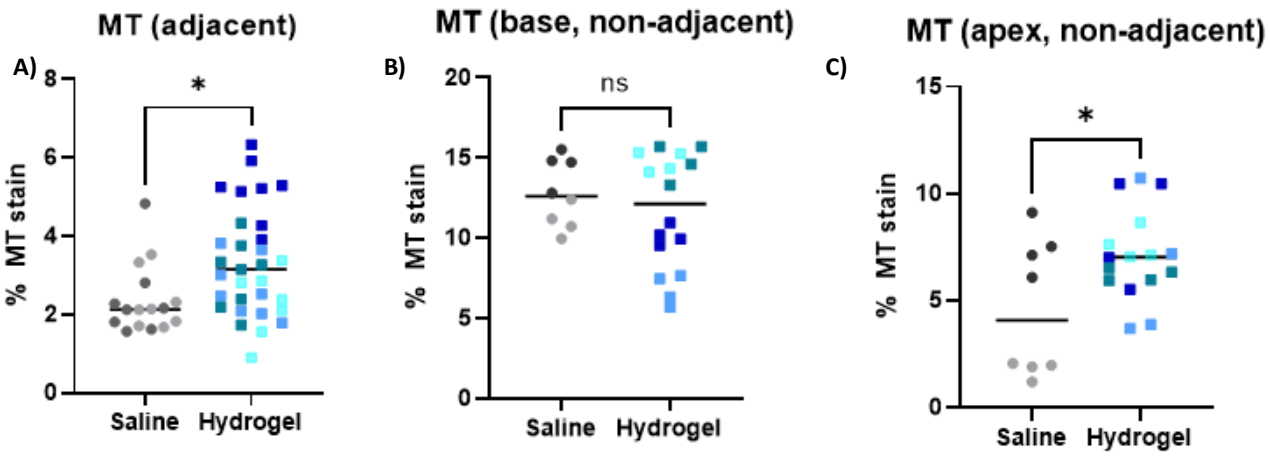


**Figure 2.2: Masson Trichrome Quantification of Non-Adjacent Sites of Injection on 2019 Cohort. (A)** Each quantification from the tissues. Each mouse has 4 quantifications and each mouse has a designated color. **(B)** Non-adjacent MT quantification near the base of the heart. **(C)** Non-adjacent quantification of tissues closer to the apex of the heart. Unpaired t test statistical analysis was performed.

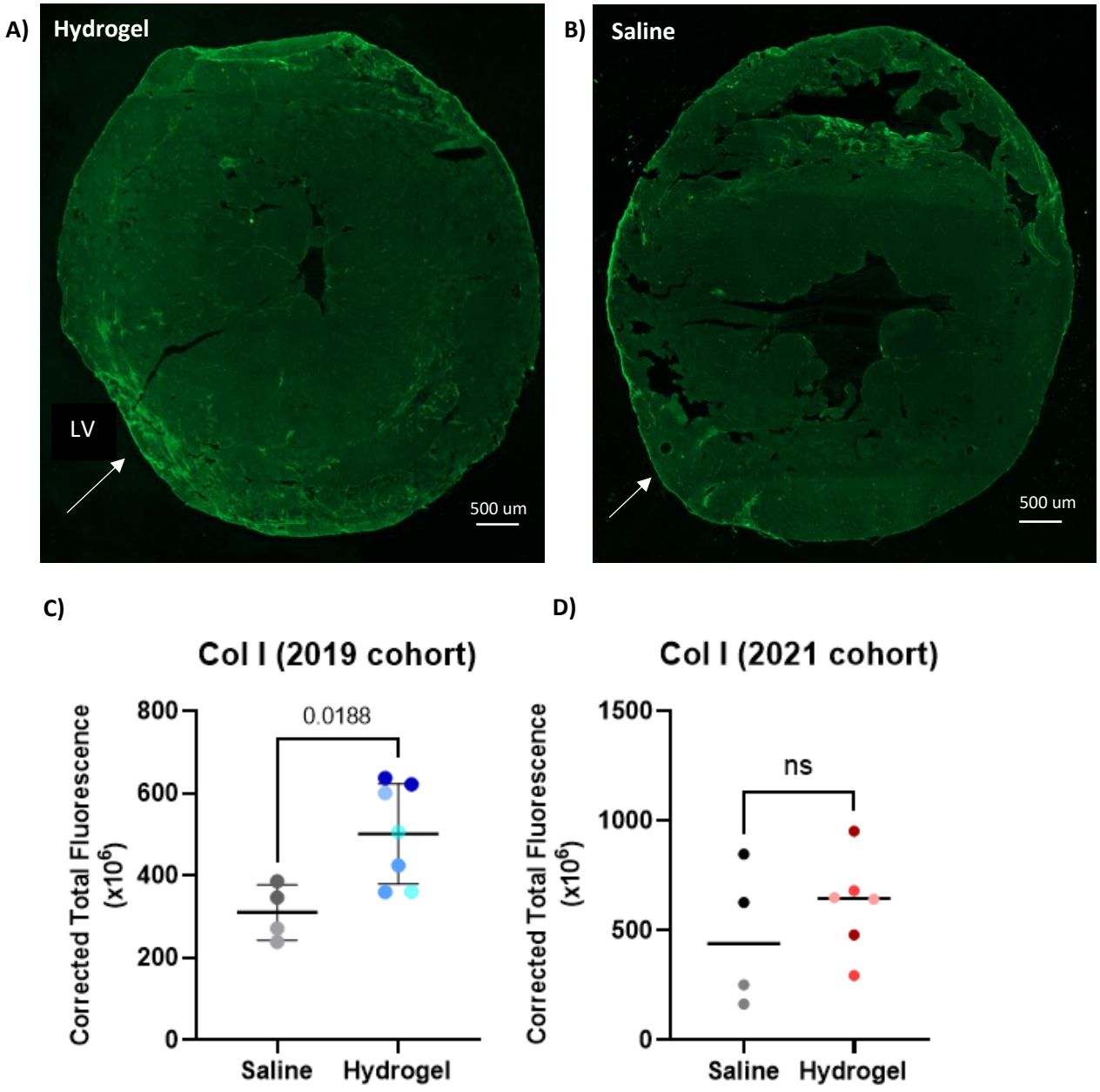


**Figure 2.3: Collagen I Levels Increased in Hydrogel-Injected Tissues From 2019 Cohort. (A)** Indirect immunofluorescent image from 2019 cohort. Mosaic image of a hydrogel injected heart tissue. Approximate injection site region in the left ventricle (LV) is indicated with arrow. **(B)** Mosaic image of a saline-injected heart tissue. Approximate injection site region in the left ventricle is indicated with arrow. **(C)** Corrected total fluorescence quantification of collagen I in the 2019 cohort. Each mouse is one color. **(D)** Corrected total fluorescence quantification of collagen I in the 2021 cohort. Each mouse is one color.

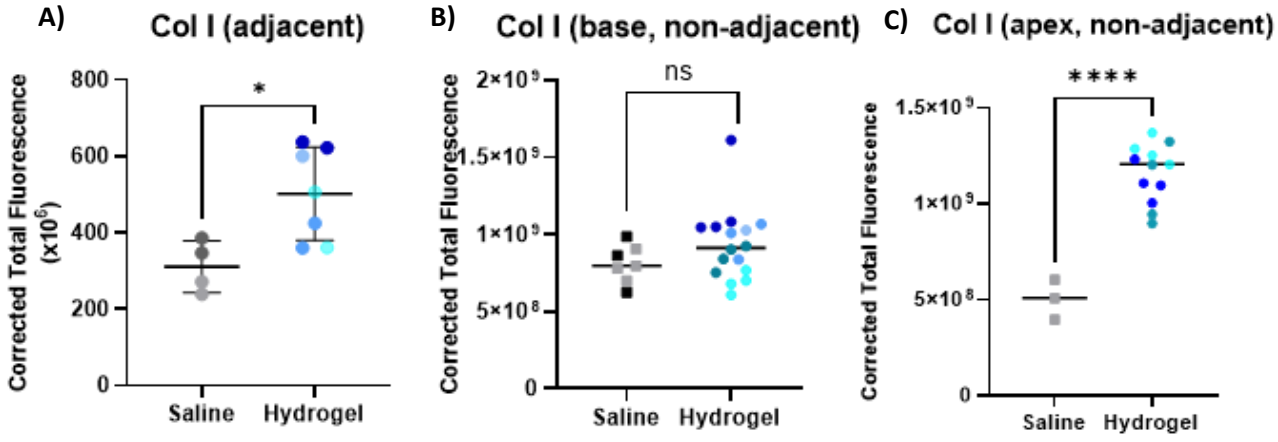


**Figure 2.4: Collagen I Quantification of Non-Adjacent Sites of Injection on 2019 Cohort. (A)** Each quantification from the tissues. Each mouse has 4 quantifications and each mouse has a designated color. **(B)** Non-adjacent collagen I quantification near the base of the heart. **(C)** Non-adjacent quantification of tissues closer to the apex of the heart. Unpaired t tests statistical analysis was performed.

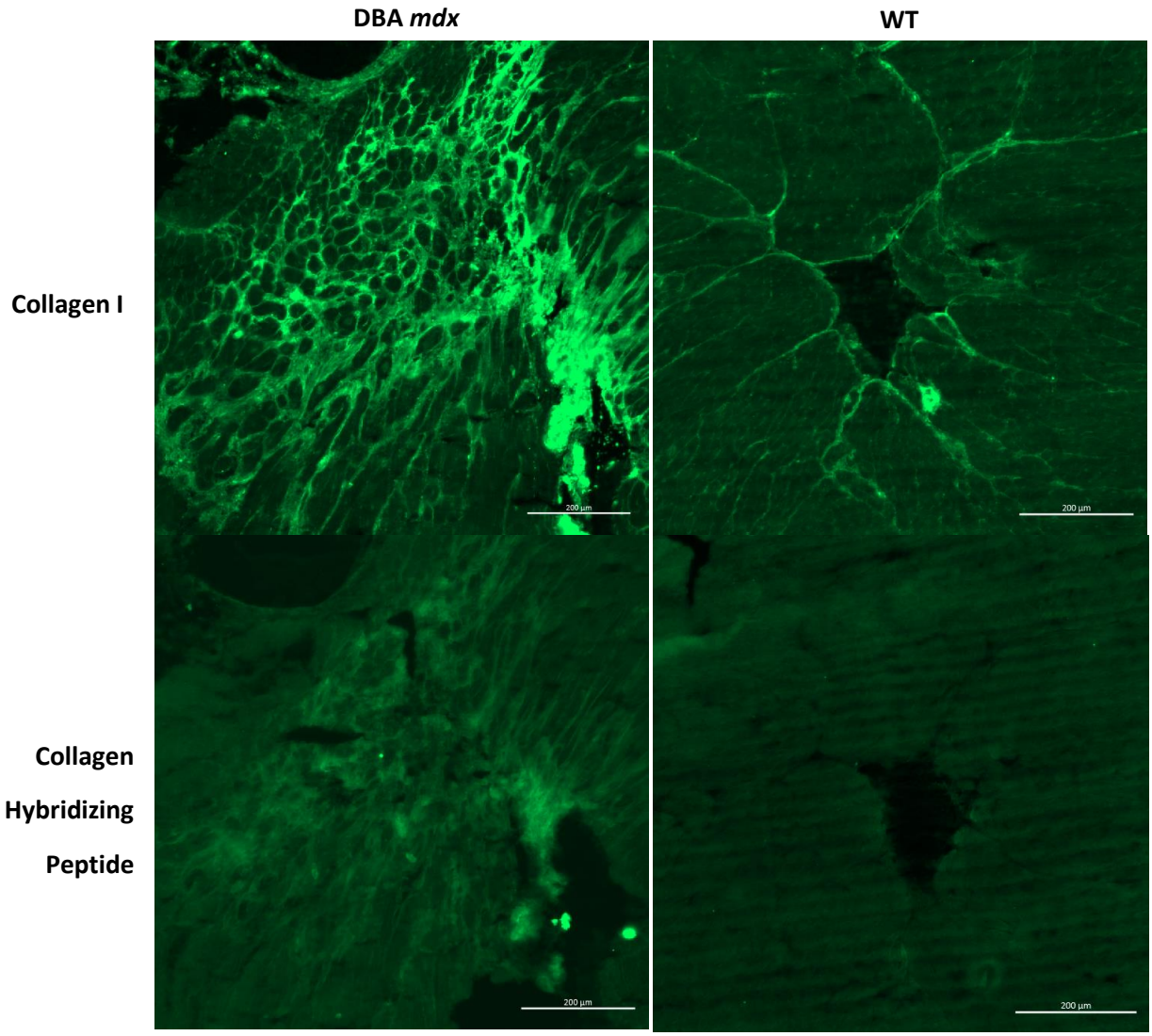


**Figure 2.5: Collagen Hybridizing Peptide Stain on Practice Tissues.** DBA *mdx* and WT hearts adjacent tissues were stained with collagen I or collagen hybridizing peptide (CHP). All scale bars at 200 uM.

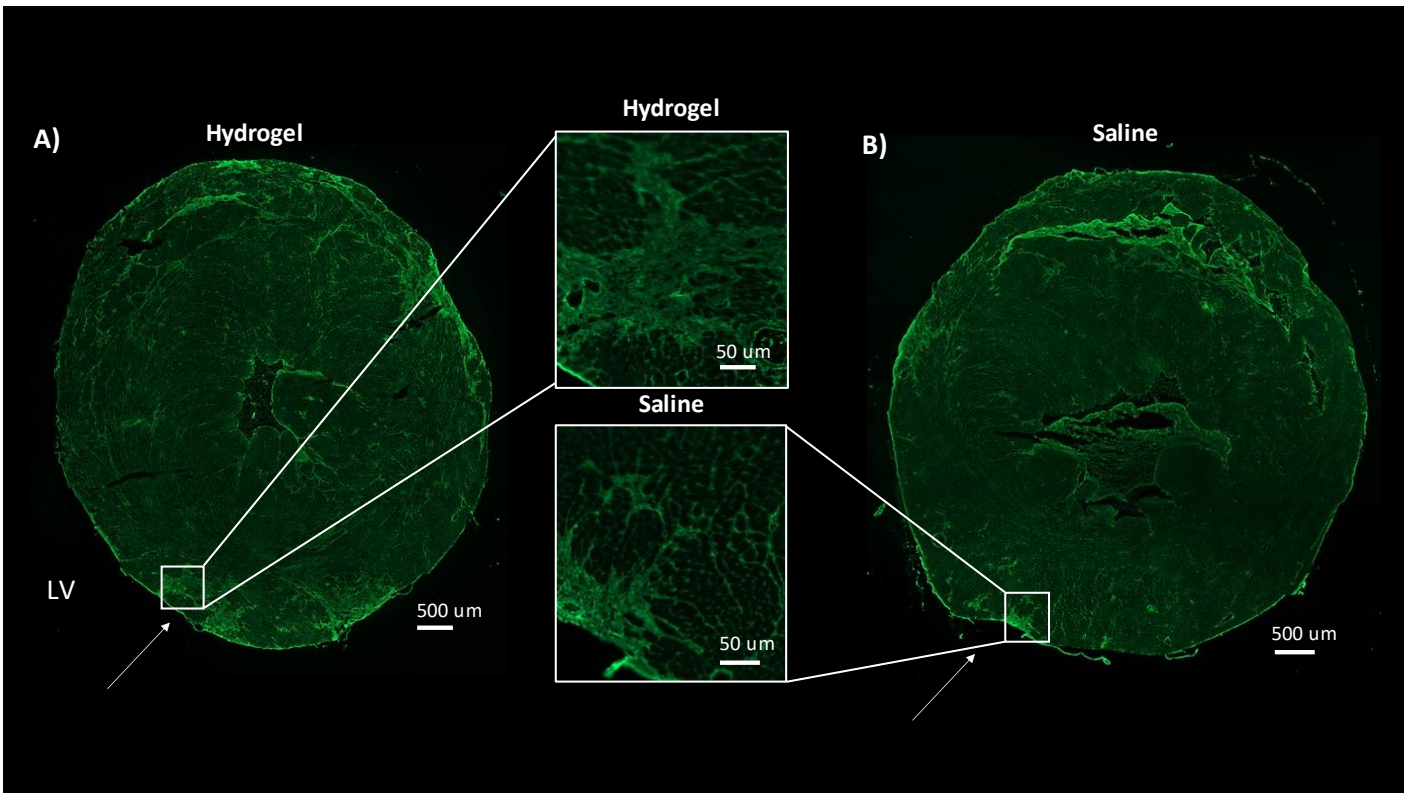


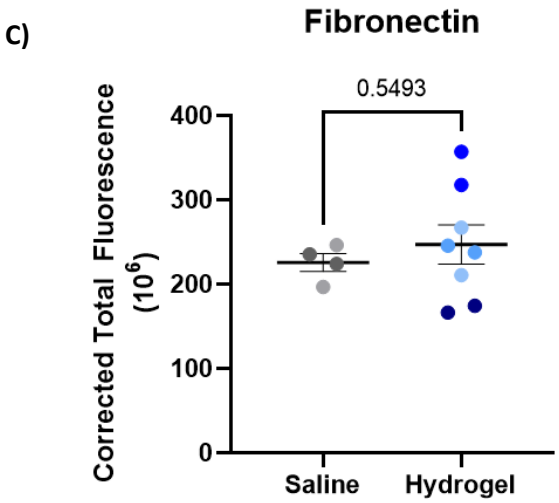


**Figure 2.6: Fibronectin Levels in Hydrogel-Injected Tissues. (A)** Indirect immunofluorescent image from 2019 cohort. Mosaic image of a hydrogel-injected heart tissue. Approximate injection site region in the left ventricle (LV) is indicated with arrow. **(B)** Mosaic image of a saline-injected heart tissue. Approximate injection site region is indicated with arrow. **(C)** Quantification of fibronectin using Corrected Total Fluorescence on 2 saline injected mice and 4 hydrogel injected mice. Each mouse had two tissues quantified.

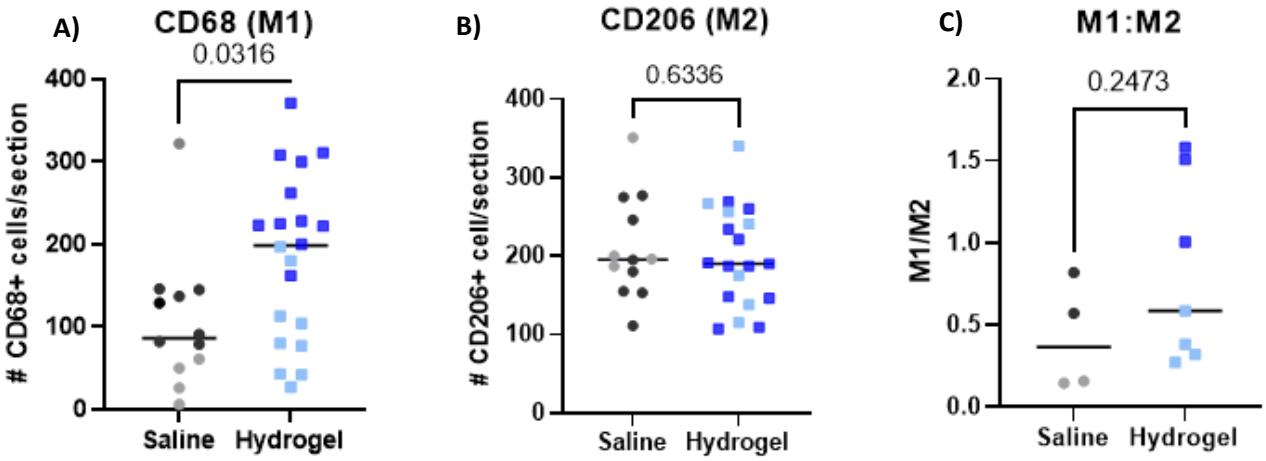


**Figure 2.7: Macrophage Quantification with a Trend of Increased M1 Population in Hydrogel Injected *mdx* Hearts.** One point represents one serial section quantified for one mouse; n = 2 saline-injected mice (2 sections per mouse), n = 4 hydrogel-injected mice (2 sections per mouse). The 2019 cohort is represented by lighter dots and the 2021 cohorts are the darker dots. **(A)** Quantification of the CD68 stain. **(B)** CD206 stain quantifications. **(C)** M1:M2 ratio = average of M1 or M2 quantifications for one mouse.

## REFERENCES


[1] F. Kamdar and D. J. Garry, “Dystrophin-Deficient Cardiomyopathy,” *J. Am. Coll. Cardiol.*, vol. 67, no. 21, pp. 2533–2546, May 2016, doi: 10.1016/J.JACC.2016.02.081.

[2] J. Holmberg and M. Durbeej, “Laminin-211 in skeletal muscle function,” *Cell Adhesion and Migration*. 2013, doi: 10.4161/cam.22618.

[3] F. Muntoni, S. Torelli, and A. Ferlini, “Dystrophin and mutations: One gene, several proteins, multiple phenotypes,” *Lancet Neurol.*, vol. 2, no. 12, pp. 731–740, Dec. 2003, doi: 10.1016/S1474-4422(03)00585-4.

[4] K. Matsumura, J. M. Ervasti, K. Ohlendieck, S. D. Kahl, and K. P. Campbell, “LETTERS TO NATURE Association of dystrophin.related protein with dystrophin.associated proteins in mdx mouse muscle,” 1992.

[5] J. A. Rafael-Fortney, J. A. Chadwick, and S. V. Raman, “Duchenne Muscular Dystrophy Mice and Men,” *Circ. Res.*, 2016, doi: 10.1161/circresaha.116.308402.

[6] E. M. Yiu and A. J. Kornberg, “Duchenne muscular dystrophy,” 2015, doi: 10.1111/jpc.12868.

[7] L. M. Ward and D. R. Weber, “Growth, pubertal development, and skeletal health in boys with Duchenne Muscular Dystrophy,” *Curr. Opin. Endocrinol. Diabetes. Obes.*, vol. 26, no. 1, p. 39, Feb. 2019, doi: 10.1097/MED.0000000000000456.

[8] J. Leor, Y. Amsalem, and S. Cohen, “Cells, scaffolds, and molecules for myocardial tissue engineering,” *Pharmacol. Ther.*, vol. 105, no. 2, pp. 151–163, Feb. 2005, doi: 10.1016/J.PHARMTHERA.2004.10.003.

[9] J. L. Ungerleider and K. L. Christman, “Concise Review: Injectable Biomaterials for the Treatment of Myocardial Infarction and Peripheral Artery Disease: Translational Challenges and Progress,” *Stem Cells Transl. Med.*, vol. 3, no. 9, p. 1090, Sep. 2014, doi: 10.5966/SCTM.2014-0049.

[10] M. T. Spang and K. L. Christman, “Extracellular matrix hydrogel therapies: In vivo applications and development,” *Acta Biomater.*, vol. 68, pp. 1–14, Mar. 2018, doi: 10.1016/J.ACTBIO.2017.12.019.

[11] J. M. Singelyn *et al.*, “Catheter-deliverable hydrogel derived from decellularized ventricular extracellular matrix increases endogenous cardiomyocytes and preserves cardiac function post-myocardial infarction,” *J. Am. Coll. Cardiol.*, 2012, doi: 10.1016/j.jacc.2011.10.888.

[12] S. B. Seif-Naraghi *et al.*, “Safety and efficacy of an injectable extracellular matrix hydrogel for treating myocardial infarction,” *Sci. Transl. Med.*, 2013, doi: 10.1126/scitranslmed.3005503.

[13] J. W. Wassenaar *et al.*, “Evidence for mechanisms underlying the functional benefits of a myocardial matrix hydrogel for post-MI treatment,” *J. Am. Coll. Cardiol.*, 2016, doi: 10.1016/j.jacc.2015.12.035.

[14] J. H. Traverse *et al.*, “First-in-Man Study of a Cardiac Extracellular Matrix Hydrogel in Early and Late Myocardial Infarction Patients,” *JACC Basic to Transl. Sci.*, vol. 4, no. 6, p. 659, Oct. 2019, doi: 10.1016/J.JACBTS.2019.07.012.

[15] J. M. Singelyn, J. A. DeQuach, S. B. Seif-Naraghi, R. B. Littlefield, P. J. Schup-Magoffin, and K. L. Christman, “Naturally derived myocardial matrix as an injectable scaffold for

cardiac tissue engineering," *Biomaterials*, 2009, doi: 10.1016/j.biomaterials.2009.06.045.

[16] Y. Yue, J. W. Skimming, M. Liu, T. Strawn, and D. Duan, "Full-length dystrophin expression in half of the heart cells ameliorates β-isoproterenol-induced cardiomyopathy in mdx mice," *Hum. Mol. Genet.*, 2004, doi: 10.1093/hmg/ddh174.

[17] Q. Jallerat and A. W. Feinberg, "Extracellular Matrix Structure and Composition in the Early Four-Chambered Embryonic Heart," *Cells*, vol. 9, no. 2, Jan. 2020, doi: 10.3390/CELLS9020285.

[18] L. Parisi, A. Toffoli, B. Ghezzi, B. Mozzoni, S. Lumetti, and G. M. Macaluso, "A glance on the role of fibronectin in controlling cell response at biomaterial interface," *Jpn. Dent. Sci. Rev.*, vol. 56, no. 1, p. 50, Dec. 2020, doi: 10.1016/J.JDSR.2019.11.002.

[19] S. Zanotti *et al.*, "Anti-fibrotic effect of pirfenidone in muscle derived-fibroblasts from Duchenne muscular dystrophy patients," *Life Sci.*, vol. 145, pp. 127–136, Jan. 2016, doi: 10.1016/J.LFS.2015.12.015.

[20] W. S. To and K. S. Midwood, "Plasma and cellular fibronectin: distinct and independent functions during tissue repair," 2011. doi: 10.1186/1755-1536-4-21.

[21] J. E. Bishop, G. J. Laurent, and J. E. Bishop, "Collagen turnover and its regulation in the normal and hypertrophying heart," 1995. [Online]. Available: https://academic.oup.com/eurheartj/article/16/suppl_C/38/549939.

[22] J. Hwang *et al.*, "Molecular assessment of collagen denaturation in decellularized tissues using a collagen hybridizing peptide," *Acta Biomater.*, vol. 53, pp. 268–278, Apr. 2017, doi: 10.1016/J.ACTBIO.2017.01.079.

[23] T. D. Johnson and K. L. Christman, “Injectable hydrogel therapies and their delivery strategies for treating myocardial infarction,” *https://doi.org/10.1517/17425247.2013.739156*, vol. 10, no. 1, pp. 59–72, Jan. 2012, doi: 10.1517/17425247.2013.739156.

[24] J. D. Hunter, T. D. Johnson, R. L. Braden, and K. L. Christman, “Injectable ECM<IndexTerm ID="ITerm2">Scaffolds</IndexTerm> for Cardiac Repair,” pp. 255–268, 2022, doi: 10.1007/978-1-0716-2261-2_17.

[25] T. Yamaoka and T. Hoshiba, “16 Biomaterials Science Series No. 6 Decellularized Extracellular Matrix: Characterization, Fabrication and Applications Edited,” 2020, doi: 10.1039/9781788015998-00116.

[26] J. Morroni *et al.*, “Inhibition of PKCθ Improves Dystrophic Heart Phenotype and Function in a Novel Model of DMD Cardiomyopathy,” *Int. J. Mol. Sci.*, vol. 23, no. 4, Feb. 2022, doi: 10.3390/IJMS23042256.

[27] J. Morroni *et al.*, “Accelerating the Mdx Heart Histo-Pathology through Physical Exercise,” 2021, doi: 10.3390/life11070706.